

Supporting information:

Reversible activation of pH-sensitive cell penetrating peptides attached to gold surfaces

Joe E. Baio, Denise Schach, Adrian V. Fuchs, Lars Schmüser, Nils Billecke, Christoph Bubeck, Katharina Landfester, Mischa Bonn, Michael Bruns, Clemens K. Weiss, and Tobias Weidner

1. Preparation of GALA-Cys

All Fmoc-protected L-amino acids and preloaded resin (Fmoc-Gly-Wang resin, 100-200 mesh, loaded 0.79 mmol·g⁻¹ or 0.30 mmol·g⁻¹) for SPPS were purchased by Novabiochem (Merck). The purity of the commercial amino acids was ≥ 98%. N-[(1H-benzotriazol-1-yl)(dimethylamino)methylene]-N-methyl-methanaminium hexafluoro-phosphate N-oxide (HBTU, Novabiochem), ethyl cyano-glyoxylate-2-oxime (Oxyma Pure, Merck, ≥98%), N,N-diisopropylethylamine (DIEA, Fluka, ≥98%), trifluoroacetic acid (TFA, Acros, 99%), triisopropylsilane (TIS, Alfa Aesar, 99%), N-methyl-2-pyrrolidone (NMP, BDH, 99%), piperazine (Merck, ≥99%), and all solvents were used as received.

1.1 Synthesis

The peptide sequences were prepared using standard solid-phase Fmoc chemistry with a microwave assisted automated peptide-synthesizer (Liberty, CEM). The parameters used for coupling and deprotection steps are mentioned below and relate to 0.1 mmol of peptide.

Coupling was achieved using under 300 s of microwave heating, with a temperature reaching and stabilized at 75 °C after around 90 s, with Oxyma Pure as activator (5 equivalents), DIEA as base (10 equivalents) and amino acid (5 equivalents). Then a first deprotection stage of 30 s (temperature reaching around 50 °C at the end) followed by a second cycle for 180 s (temperature 75 °C) with a 20 wt% solution of piperazine in DMF. The resin was washed 3 to 5 times between each coupling or deprotection step. Cleavage of peptide from the resin was performed using a mixture of TFA/TIS/H₂O (95%/2.5%/2.5%) for 15 h at ambient temperature. After filtration, the peptides were precipitated and centrifuged three times in cold diethyl ether, and dried over vacuum.

To exchange the TFA with DCI counter ions 10 mg of the GALA-Cys were solubilized in 20 µL deuterated 2,2,2-trifluoroethanol (TFE) with 40 µL of D₂O (pH* 2.3, DCI) while being placed in an ultrasonic bath for 15 min. To support the deuteration of the N–H groups of the peptide bonds the vial was heated up to 38° C in a tempered shaker for 2 h. After deep-freezing the solution in liquid nitrogen the peptide was freeze-dried overnight. This procedure was repeated three times.

1.2 Peptide Characterization

NMR

¹H NMR spectra were recorded on Bruker DRX spectrometer (300 MHz) at 298.7 K in DMSO-d₆.

MALDI-TOF

MALDI-TOF MS analyses were obtained on a Bruker-Daltonics Reflex-TOF, in reflex (peptide) or linear (polymer and conjugates) mode. The acceleration voltage was 20 kV in both cases. The samples (solid state) were incorporated in 2,5-dihydroxy benzoic acid (DHB) matrix and desorbed with a nitrogen laser ($\lambda = 337$ nm).

HPLC

HPLC was performed a gradient of THF/0.01% TFA in H₂O employing a reversed phase HD C8 column (Macherey-Nagel) using a series 1100 pump (Hewlett Packard) and an auto 1200 series sampler (Agilent Technologies). Substances were detected by a UV-Vis detector S-3702 (Soma) at 220 nm. Flow was 1 mL·min⁻¹ and the concentration of the sample 1 mg·mL⁻¹.

Fourier transform infrared spectroscopy

FTIR spectra of Gala-Cys in solution at pH = 12 and 3 (see Figure S1) were recorded in transmission mode to control whether the mechanism of pH triggered helix-coil transition is also valid for this variant of GALA peptide. The spectra were compared to those of pure GALA in solution.¹ In brief, bands related to dedeuterated Glu side chains at pH = 12 are visible near 1567 cm⁻¹ and 1406 cm⁻¹.² At pH = 3 a broad band around 1706 cm⁻¹ appears in the spectrum which is related to the deuteration of Glu.² From this result we can conclude that the fully dedeuterated or deuterated states of Glu are achieved for pH =12 or 3, respectively. As observed for the original GALA sequence the center of the

amide I' band shifts from 1652 to 1642 cm^{-1} verifying the helix-coil transition upon increasing pH. The band assignments are summarized in Table S1. The data show that GALA-Cys behaves in complete analogy to the unmodified GALA peptide.

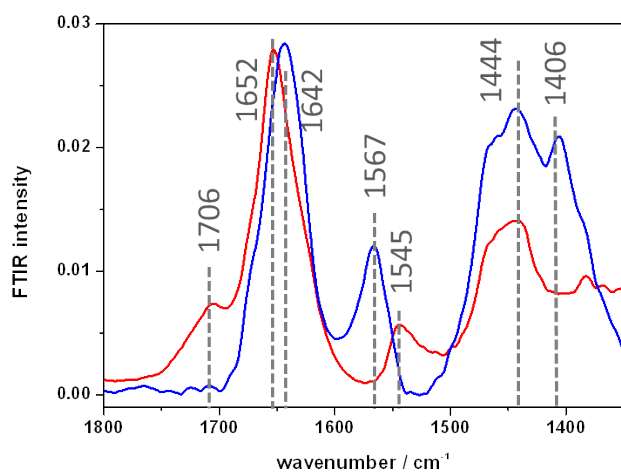


Figure S1: Transmission FTIR spectra of 0.2 mg / 20 μl GALA-Cys in D_2O containing 0.1 M K_2HPO_4 at pH = 12 (blue trace) and pH = 3 (red trace).

Table S1: FTIR band assignments

Band position / cm ⁻¹	Assignment
1706	deuterated Glu
1652	α -helix (amide I')
1642	random structure (amide I')
1567	dedeuterated Glu (antisym.)
1545	amide II
1444	amide II'
1406	dedeuterated Glu (sym.)

2. Surface attachment

The GALA-Cys-SAM formation on a closed planar gold film was followed with surface plasmon resonance (SPR), electrochemical impedance spectroscopy (EIS), surface-enhanced infrared absorption spectroscopy (SEIRAS), and X-ray photoelectron spectroscopy (XPS).

2.1 SPR

SPR angle scans were taken before and after monolayer formation (Figure S2 A). A quantitative analysis of the plasmon shape assuming a four-layer model (prism/chromium/gold/peptide, see table S2) and a refractive index of $n = 1.45$ for the protein³ yields a peptide layer thickness of $1.5 \text{ nm} \pm 0.5 \text{ nm}$. A thick GALA-cys multilayer – as suspected earlier by Goormaghtigh et al. for unmodified GALA at interfaces¹ – can therefore be excluded here. The thickness value indicates a strongly inclined adsorption geometry. The tilt angle of the peptide helix can be estimated to be $\sim 20^\circ$ with respect to the surface assuming a peptide length of $\sim 5 \text{ nm}$.

Table S2: Fit parameters used to estimate the layer thickness of the GALA-Cys SAM with SPR.

Layer	thickness / Å	n	κ
LaSFN9 prism / LaSFN9 template	0.0*	1.85*	0.00*
Cr	25.9	2.45*	3.28*
Au	567.1	0.17*	3.54*
peptide SAM	15.0	1.45*	0.00*
Aqueous buffer	0.0*	1.33*	0.00*

*Literature values which were fixed in the fits.

2.2 EIS

The EIS Bode plot shown in Figure S2 B was analyzed using the equivalent circuit illustrated in Figure S2 C and is a standard method to analyze thin organic layers such as lipid membranes.⁷ The analysis yielded resistance and effective capacitance values^{4, 5} for the GALA peptide SAM of $10.78 \text{ M}\Omega\text{cm}^{-2}$ and $4.95 \mu\text{F cm}^{-2}$, respectively (Table S3). Compared to equivalent parameters obtained from comparable systems such as solid-supported lipid membrane architectures, we can conclude the protein layer is very dense.⁸ In addition, the obtained value of 0.97 for n (table S4) indicates the peptide film is homogeneous.⁸ This is supported by atomic force microscopy (AFM) images recorded before and after the SAM-formation do not show any structural alteration of the surface, such as aggregates, particles or domains (see 2.4).

Table S3 Summary of EIS-determined fit parameters* for GALA-CYS on gold. The capacitance C, the resistance R, and the layer thickness d were obtained from fitting the EIS and the SPR data, respectively.

	GALA-Cys SAM
Film thickness/nm	1.5 (0.5)
Capacitance/ $\mu\text{F cm}^{-2}$	4.95 (0.15)
Resistance/ $\text{M}\Omega \text{ cm}^{-2}$	10.78 (1.41)

* Experimental errors in parentheses.

Table S4 Fit parameters* obtained by fitting a R(RQ) equivalent circuit to the admittance data.

EIS fit parameters	Value
$R_{\text{buffer}} / \Omega \text{ cm}^2$	17.1 (0.6)
$R_{\text{SAM}} / \text{M}\Omega \text{ cm}^{-2}$	10.8 (1.4)
$Q_{\text{SAM}} / \mu\Omega^{-1} \text{ cm}^{-2}\text{s } \alpha$	6.5 (0.3)
α_{SAM}	1.0 (0.4)

* Experimental errors in parentheses.

2.3 SEIRAS

For the SEIRAS measurement two mirrors were placed in the optical path to couple the IR beam into a right-angle Si ATR crystal at 45°. To the upper surface a 7 nm gold island film was evaporated before, serving as the substrate and providing a surface enhancement effect at the same time. A sample temperature controlled flow cell with a temperature stability of $< \pm 0.1^\circ\text{C}$ was adjusted to the surface. A reference spectrum with the afore-mentioned buffer solution at pH = 9 was taken before peptide adsorption. The GALA-cys solution was added to the sample cell and difference spectra were recorded right after the injection to follow the adsorption kinetics. After the adsorption was completed the sample cell was flushed with fresh buffer. SEIRAS was used to study the adsorption kinetics of GALA-Cys on a gold island film in D₂O at pH = 9 (Figure S2 D). The difference spectra with respect to the spectrum of the surface before peptide addition were taken between 2 (black) and 100 min (green) after injection of the peptide solution to the measurement cell. The growth of distinct bands at 1408, 1564 and 1630-1640 cm⁻¹, referring to symmetric and anti-symmetric stretch vibrations of the carboxyl-group of the glutamic acid and amide I' band, respectively, reflect the increasing peptide concentration at the surface. At the same time, a negative band to the blue side of the amide I' band decreases in amplitude with adsorption time. This band, either a water bending mode, an OHD bending mode or a combination, originates from the loss of water at the very interface being replaced by the peptide layer. We do not expect a high water content in the prepared D₂O buffer, however the difference measurements are extremely sensitive to small changes in concentration at the surface.⁹ Due to this interfering

band, we are not able to isolate the amide I' mode in the spectra. We can, however, monitor the amide I' band intensity relative to the minimum on its low frequency side, as illustrated by the in Figure 2 D. The length of that arrow has been plotted vs. adsorption time (Figure S2 E, red) and compared to the adsorption kinetics followed by SPR (Figure S2 E, black). Both curves show that the entire adsorption process takes approximately 40 min. The SPR kinetics shows a further linear increase for longer adsorption times, whereas the SEIRAS kinetics plateaus after 40 min. This might be explained by unspecific adsorption onto the closed layer to which SEIRAS is less sensitive. We found that rinsing the sample cell with fresh buffer solution after 40 min inhibited further unspecific adsorption.

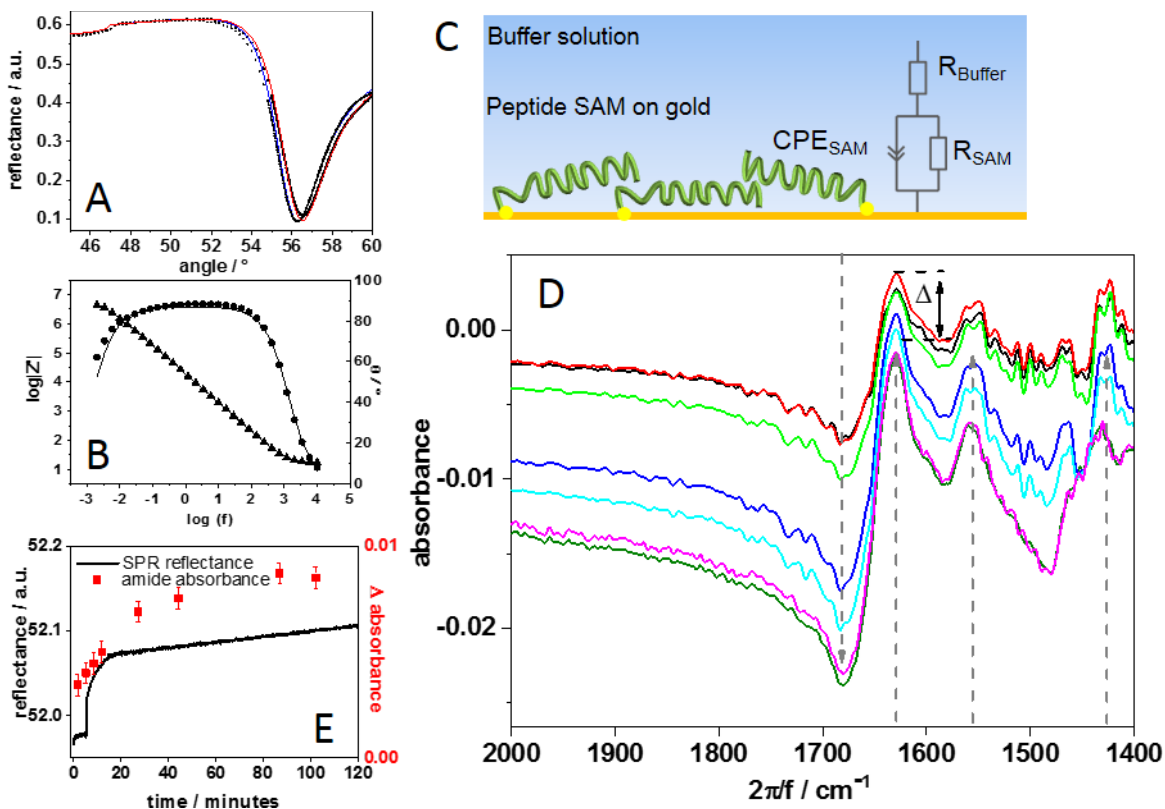


Figure S2. Characterization of the GALA-SAM growth. (A) SPR angle scans were measured before (blue) and after (red) SAM formation. (B) EIS Bode Plot for GALA SAMs at pH = 9 to characterize the electrochemical film properties. (C) Illustration of the equivalent circuit model used for the Bode plot analysis. (D) SEIRAS difference spectra measured during the self-assembly of GALA on gold at pH = 9 (2 min: black), 5 min: red, 9 min: light green, 27 min: blue, 44 min: light blue, 86 min: pink, 100 min: green (B). A decreasing negative band to the high frequency side of 1650 cm^{-1} refers to the loss of water near the very surface. Rising features around 1650 , 1564 , and 1408 cm^{-1} indicate protein binding. (E) GALA-cys adsorption kinetics determined with SPR (black) and the increasing intensity of the SEIRAS amide I' band.

2.4 Atomic force microscopy (AFM)

The AFM measurements were performed using a Dimension3100 CL Scanning Probe Microscope in the tapping mode. An OMCLAC160 TS-W2 (silicon coating, resonance frequency: 300kHz in air, tip radius 7nm) was used to scan several spots on different parts of the sample surface at a surface area of 1 μm^2 .

AFM measurements were performed to characterize the gold surfaces before and after SAM formation (Figure S3). The topographic AFM images of both surfaces do not show any significant difference and the grain structures are remained after SAM formation. The phase images and phase RMS values, however show differences in smoothness which can be attributed to different physical properties of bare gold and peptide layers (Table S5).

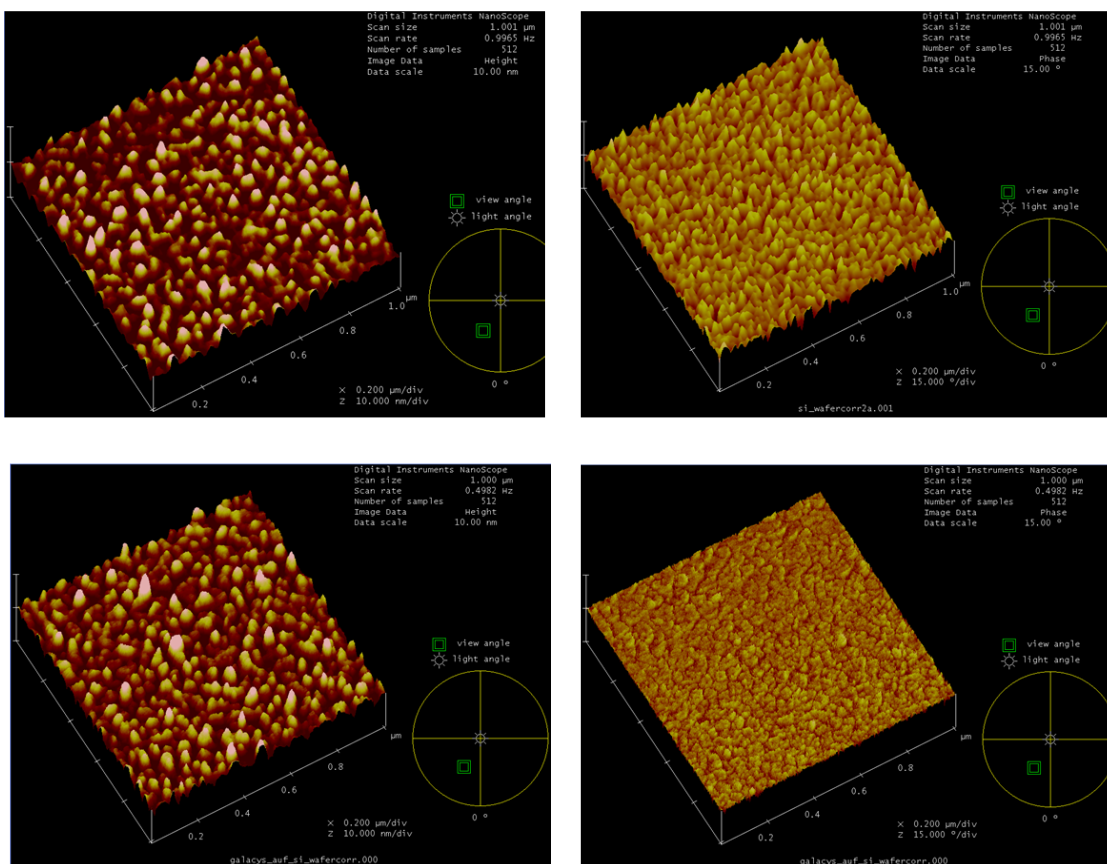


Figure S3: AFM topography of a 55 nm thick gold film as used for SPR and EIS measurements before (upper left panel) and after SAM formation (lower left panel). According AFM phase images before (upper right panel) and after SAM formation (lower right panel).

Table S5: AFM topographic and phase RMS for bare gold before and after SAM formation.

	bare gold	gold + SAM
topographic RMS / nm	0.97	1.16
phase RMS / °	1.43	0.53

2.4 XPS

Quantitative characterization of the composition and chemical integrity of GALA-cys films are provided by XPS. The inferred composition, averaged over three samples of rinsed and dried GALA-cys films is reported in Table S6. The surface composition showed the expected presence of carbon, nitrogen and oxygen. The results are in good agreement with the theoretical composition of GALA-cys and also previously reported compositions of protein monolayers and with theoretically expected values.⁶⁻¹³ Sulfur, related to the cysteine group, was not detected. This is most likely explained by three factors: (i) the low sulfur concentration in the peptide (0.5 atomic %), (ii) the large footprint of the tilted GALA peptides on the surface means a low sulfur surface density and (iii) attenuation of the sulfur XPS signal due to inelastic scattering from the rest of the peptide. Unbound or oxidized sulfur – indicators of loosely bound or degraded peptide linkers in the film – were not observed.

Table S6: Summary of XPS determined elemental composition^a for GALA-CYS on gold.

	C	N	S	O
Theor. composition	63.1	15.5	0.5	20.9
Exp. composition	70.7(2.1)	11.1(2.0)	n.d. ^b	18.2(1.1)

^a Values in atomic % with experimental errors in parentheses. ^b Not detected.

The pKa of GALA at Au surfaces

The pK_a value of a species at an interface can differ significantly from the respective bulk or solution state values. We used SEIRAS to follow the protonation of the glutamic acid sites as a function of solution pH (Figure S4). The solution was titrated from basic pH to acidic pH. The respective spectra of the 1564 cm^{-1} mode related to the glutamic acid carboxylate group are shown in Figure S4 (top panel). Upon titration to acidic pH the 1564 cm^{-1} band decreases stepwise. When plotting the intensity of the band at 1564 cm^{-1} relative to the minimum on the high frequency side (indicated by the arrow) vs. the pH value, one can follow the deprotonation of the carboxylate groups (Figure S4, bottom). A sigmoidal curve has been fitted to the data points to determine the midpoint, the average pK_a value of Glu sites. We found the pK_a value of the attached GALA to be 5.5, slightly lower than the pK_a value reported previously for bulk solution of ~ 6 .⁴⁵ This slightly lower pK_a value for GALA-cys at the surface is most likely explained by differences between the interfacial and bulk pH value, as well as possibly a reduced accessibility of the Glu sites on the surface. A further difference between solution- and surface state GALA is the occurrence of aggregation in solution, absent at the surface. We repeated the experiment in a reverse order, moving from acidic to basic pH value and observed the same trend without any sign of hysteresis. Hysteresis in a pH titration has been associated with peptide aggregation. We have observed such a hysteresis in a pH titration of the dissolved peptide in solution. For the low to high pH titration we observed very similar titration curves and pK_a values as shown in here, however, for high to low pH titrations we observed steep curves with a pK_a near 6,

indicating collective transitions typical for aggregates. Lateral aggregation of GALA at the interface can therefore be ruled out here, most likely because of the covalent surface attachment. This result is also supported by the EIS results discussed above and atomic force microscopy images, which did not show protein aggregates.

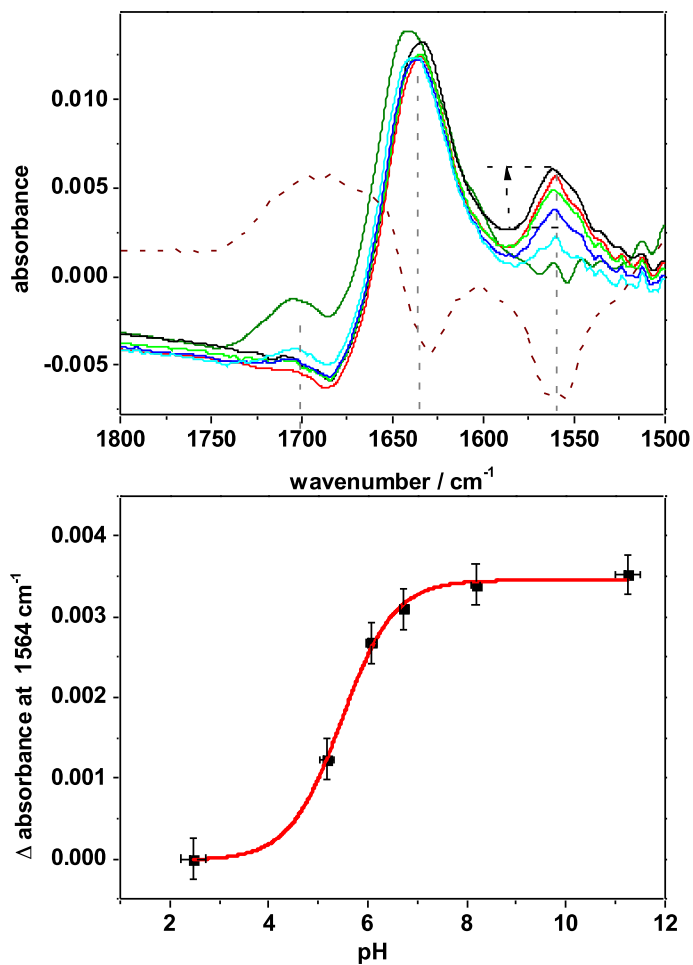


Figure S4. (Top) Surface-enhanced ATR-FTIR difference spectra – with respect to the surface before the peptide was added – titrated from basic pH stepwise to acidic pH (pH* = 11.25 (black), 8.18 (red), 6.73 (light green), 6.08 (blue), 5.18 (light blue), 2.48 (green). Bands referring to the Glu-carboxyl and -carboxylate group appear at 1700 and 1664 cm⁻¹, respectively. Upon titration to low pH the low-frequency band declines whereas the high-frequency band increases. The difference spectrum (dark red) (fully protonated - fully deprotonated) indicates the loss of the 1564 cm⁻¹ band, the blue shift of the amide I' band, and the gain of the band at 1700 cm⁻¹ upon lowering the pH. (Bottom) Titration curve based on the relative intensity of the 1564 cm⁻¹ band (as indicated by the arrow in the top panel) vs solution pH. The fit of a sigmoidal curve to the data yields a midpoint of pH* = 5.5.

SFG Fitting Details

Lorentzian peak shapes were fitted to SFG spectra by the following expression:

$$I_{SFG} \propto |X^{(2)}|^2 \propto \left| A_{NR} e^{-i\phi_{NR}} + \sum_n \frac{A_n}{\omega_n - \omega_{IR} - i\Gamma_n} \right|^2$$

Here, A_{NR} is the amplitude and ϕ_{NR} the phase of nonresonant signal, A_n is the amplitude of resonant signal, ω_n is the resonant frequency, ω_{IR} is the infrared frequency, and Γ_n is the width of transition. Fitting results are summarized in Table S7.

Table S7: Band fitting parameters for the SFG spectra taken from GALA-cys on Au at the various experimental pH's under ppp polarization conditions

	A_{NR}	φ_{NR}	ω_n (cm ⁻¹)	Γ_n (cm ⁻¹)	A_n (a.u.)
pH 3	0.7	1.3	1650	50	36.2
			1630	50	-7.1
			1675	50	8.6
pH 6	0.8	1.3	1650	50	53.7
			1630	50	-12.3
			1675	50	5.4
pH 9	1.0	1.3	1650	50	3.6
			1630	50	6.6
			1675	50	-3.9
pH 12	0.9	1.3	1650	50	-0.1

1630	50	8.1
1675	50	2.3

Fluorescence microscopy

Fluorescence microscopy was used to test the membrane perturbation activity of surface bound GALA-Cys triggered by low pH. Large unilamellar vesicles (LUV) with 99.8% dipalmitoylphosphatidylcholine (DPPC) and 0.2% 1,2-dipalmitoyl-sn-glycero-3-phosphoethanolamine-N-(lissamine rhodamine B sulfonyl) (16:0 Liss Rhod PE) were adsorbed to gold and GALA-Cys surfaces. The fluorescent lipids of the outer leaflet, which were exposed to the bulk medium were reduced and thereby quenched by sodium dithionite (DTT). Thus, only the inner leaflet of the LUVs contributed to the fluorescence intensity measured with fluorescence microscopy. After membrane perturbation through GALA-Cys also the inner leaflet becomes accessible to DTT and becomes reduced and quenched. Therefore the accessibility of DTT to the inner leaflet was a direct evidence for membrane perturbation due to GALA-Cys.

To get a clear boundary between the uncoated gold surface and the SAM of GALA-Cys the gold coated glass substrate was only half covered with GALA-Cys incubation buffer (0.3 mg/ml pH 9.5) during SAM formation. Afterwards the glass slide was thoroughly rinsed with water to remove nonspecific adsorbed GALA-Cys molecules.

Vesicle preparation has been described in detail elsewhere.¹⁴ Briefly, lipids dissolved in chloroform were dried in a glass vial with a flowing nitrogen stream to form a thin lipid film. The thin film was further dried in a vacuum chamber for 3 hours to remove remaining solvent. The Lipids were resuspended in buffer (pH 9.5) by vortexing thoroughly and passed through an extruder (Miniextruder, Avanti Lipids) 11 times directly before usage. 100 μ l buffer (pH 9.5) containing 2 mg/ml LUV (99.8% DPPC and 0.2% Liss Rhod PE) was infused into the measurement chamber, a channel was created on the GALA-coated gold surface using double sided sticky tape and cover slips, allowing controlled exchange of buffer, and incubated for 1 hour. Excess lipids and dye were flushed out with three volumes of pH 9 buffer. The channel was then flushed with quencher solution at pH 9 and subsequently the buffer was exchanged with quencher solution at pH 5. After each step, three images were acquired of GALA covered- and control areas with an Olympus IX80 inverted microscope (Olympus, Hamburg, Germany) equipped with a Cy3 filter set cube (Thorlabs) using the Cell F imaging software. Care was taken to image previously unexposed areas with fixed exposure time (500 ms). The Images were processed using ImageJ.

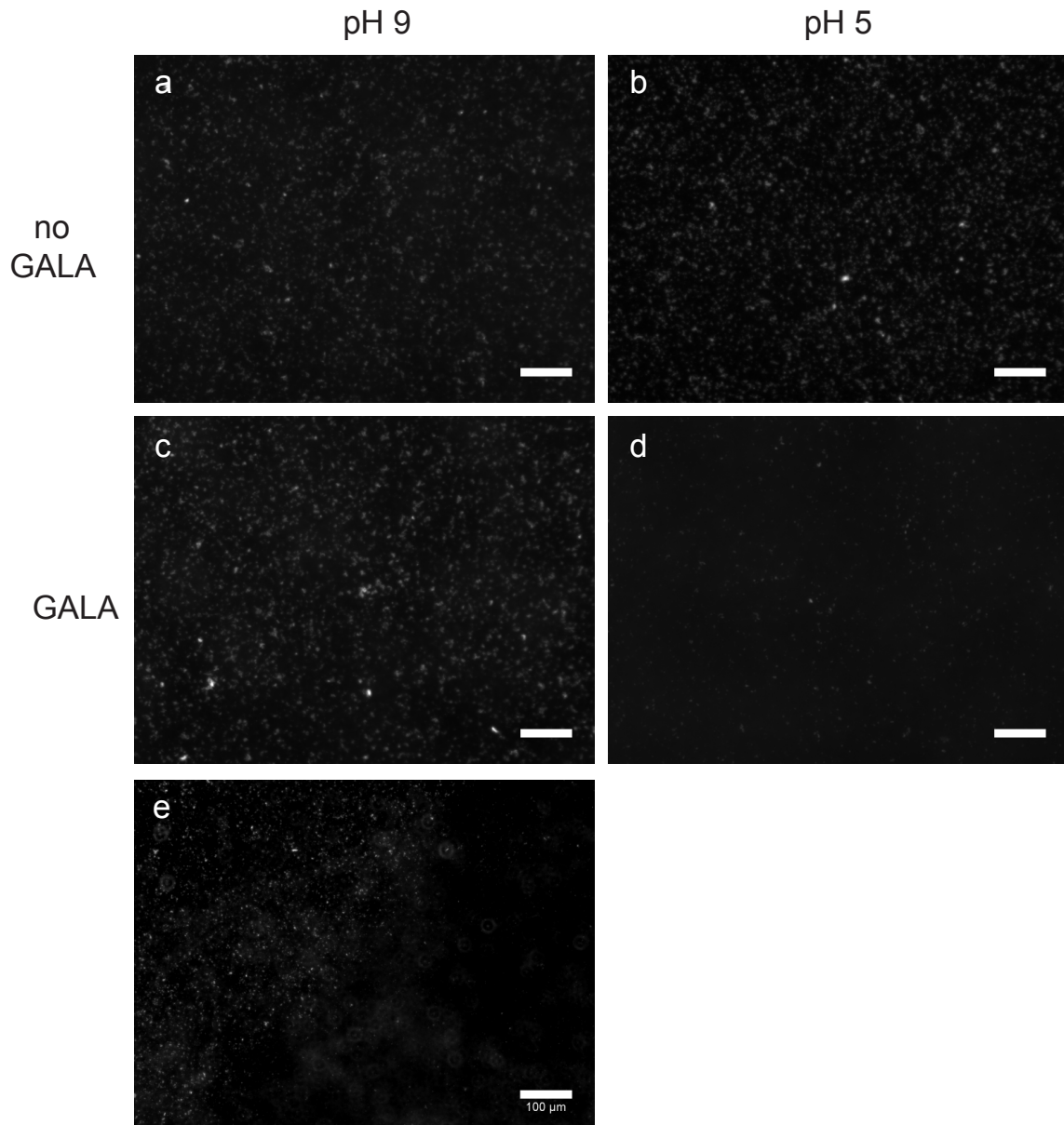


Figure S5. Images acquired directly after vesicle formation show a uniform distribution on both GALA tethered and control area at pH9 (figure S5 a,b). Dropping the pH to 5 in the presence of quencher decreased detectable fluorescence of vesicles only were GALA was tethered to the interface, but not in the control area (Figure 5 c,d). This indicates the loss of membrane integrity,

which allows interaction of quencher and rhodamine only in the presence of GALA (figure 5e).

Scale bar: 50 μm unless stated otherwise.

References:

1. E. Goormaghtigh, J. De Meutter, F. Szoka, V. Cabiaux, R. A. Parente and J.-M. Ruysschaert, *European Journal of Biochemistry*, 1991, **195**, 421-429.
2. A. Barth, *Progress in Biophysics and Molecular Biology*, 2000, **74**, 141-173.
3. N. Bunjes, E. K. Schmidt, A. Jonczyk, F. Rippmann, D. Beyer, H. Ringsdorf, P. Gräber, W. Knoll and R. Naumann, *Langmuir*, 1997, **13**, 6188-6194.
4. F. Shamsi, H. Coster, K. A. Jolliffe and T. Chilcott, *Materials Chemistry and Physics*, 2011, **126**, 955-961.
5. R. Naumann, T. Baumgart, P. Gräber, A. Jonczyk, A. Offenhäusser and W. Knoll, *Biosensors and Bioelectronics*, 2002, **17**, 25-34.
6. J. Baio, F. Cheng, D. M. Ratner, P. S. Stayton and D. G. Castner, *Journal of Biomedical Materials Research Part A*, 2011, **97**, 1-7.
7. J. E. Baio, T. Weidner, L. Baugh, L. J. Gamble, P. S. Stayton and D. G. Castner, *Langmuir*, 2012, **28**, 2107-2112.
8. J. E. Baio, T. Weidner and D. G. Castner, in *Proteins at Interfaces III State of the Art*, American Chemical Society, 2012, vol. 1120, pp. 761-779.
9. J. E. Baio, T. Weidner, G. Interlandi, C. Mendoza-Barrera, H. E. Canavan, R. Michel and D. G. Castner, *J. Vac. Sci. Technol. B*, 2011, **29**, 04D113.
10. J. E. Baio, T. Weidner, N. T. Samuel, K. R. McCrea, L. Baugh, P. S. Stayton and D. G. Castner, *J. Vac. Sci. Technol. B*, 2010, **28**, C5D1-C5D8.
11. J. S. Apte, G. Collier, R. A. Latour, L. J. Gamble and D. G. Castner, *Langmuir*, 2010, **26**, 3423-3432.
12. L. Baugh, T. Weidner, J. Baio, P. C. T. Nguyen, L. J. Gamble, P. S. Stayton and D. G. Castner, *Langmuir*, 2010, **26**, 16434-16441.
13. F. Cheng, L. J. Gamble and D. G. Castner, *Anal. Chem.*, 2008, **80**, 2564-2573.
14. R. C. MacDonald, R. I. MacDonald, B. P. M. Menco, K. Takeshita, N. K. Subbarao and L.-r. Hu, *Biochimica et Biophysica Acta (BBA) - Biomembranes*, 1991, **1061**, 297-303.